XLVI CILAMCE
VITÓRIA - ES - BRAZIL - 2025
XLVI IBERO-LATIN AMERICAN CONGRESS ON COMPUTATIONAL METHODS IN ENGINEERING

A modified creep analytical model for predicting shale well closure in abandonment and CCS/CCUS applications

Marcello Congro[1,2], Pedro A. L. P. Firme[2] and Deane Roehl[1,2]

[1]*Department of Civil and Environmental Engineering, Pontifical Catholic University of Rio de Janeiro (PUC-Rio)*
Rua Marquês de São Vicente 225, Gávea, 22451-900, Rio de Janeiro/RJ, Brazil
marcellocongro@tecgraf.puc-rio.br, plobo@tecgraf.puc-rio.br, deane@tecgraf.puc-rio.br
[2]*Multiphysics Modeling and Simulation Group, Tecgraf Institute, PUC-Rio*
Rua Marquês de São Vicente 225, Building Pe. Laércio Dias de Moura S.J., Gávea, 22451-900, Rio de Janeiro/RJ, Brazil

Abstract. Ensuring long-term well integrity is a fundamental challenge in plug and abandonment (P&A) and carbon capture, utilization, and storage (CCS/CCUS) operations. Clayey formations such as some shales exhibit time-dependent deformation. In these environments, well closure due to creep forming a geological barrier contributes to zonal isolation and long-term sealing. This study proposes a modified creep analytical model that extends the classical Barker solution, originally developed for salt, to capture the creep behavior of shales. The formulation is slightly modified in order to be consistent with creep constitutive models relevant to salt and shale geomechanics. The stress state surrounding the well right after drilling is derived using Kirsch's elastic solution, enabling a closed-form expression of the deviatoric stress. Next, creep behavior is activated, and a time-dependent exponential decay function, calibrated using numerical simulations, is introduced to capture the stress relaxation during material deformation. The resulting stress field feeds into an analytical, iterative framework for computing well radius evolution over time. Validation against numerical simulations demonstrates good agreement, underscoring the model's applicability for barrier design and integrity evaluation in well P&A and CCS/CCUS scenarios.

Keywords: Shale, creep, analytical solution, P&A.

1 Introduction

Shales are widely present in subsurface formations and are increasingly considered as potential sealing materials in well plug and abandonment (P&A) operations. Ductile, clay-rich shales exhibit time-dependent deformation, low permeability, and self-healing properties, which are generally favorable for ensuring long-term zonal isolation. The time-dependent deformation observed in such formations is commonly referred to as creep at the macroscopic scale, although mechanisms such as swelling and consolidation may also contribute to the overall deformation process, particularly given the clayey nature of the rock. As P&A practices evolve toward more robust long-term barrier qualification, the ability to understand and predict well closure over time becomes critical for assessing shale-driven barrier formation and meeting regulatory compliance.

One of the main challenges in this context lies in accurately predicting well closure (i.e., the formation of a geomechanical barrier around the casing) due to shale deformation under varying stress and temperature conditions. While sophisticated numerical models based on finite element (FE) methods are commonly employed for this purpose, their practical application is often constrained by high computational cost, reliance on commercial software, and significant data input requirements. In contrast, analytical models provide an attractive alternative for generating faster and reasonably accurate predictions with reduced complexity.

A notable example is the analytical solution developed by Barker [1] to describe creep-induced closure in

salt formations. This model assumes that the stress field around the well remains elastic and that creep deformation is driven by a constant differential stress. It offers a simplified yet powerful expression to estimate well radius evolution over time, incorporating the effects of stress, temperature, and material behavior using a combined Power and Arrhenius-type creep law. However, the direct application of Barker's solution to shales is limited, primarily due to fundamental differences in creep mechanisms and the need for shale-specific parameter calibration.

In this study, we present an adaptation of Barker's analytical framework to account for creep in shale formations, introducing key modifications in both the stress characterization and the creep formulation. The contributions of this work include: (i) the deviatoric stress driving the creep process is derived from Kirsch's elastic solution for a plate with a pressurized hole, representing the stress state immediately after drilling, an approach commonly found in rock mechanics literature such as Goodman [2] and Fjaer et al. [3]; (ii) this deviatoric stress is allowed to relax over time following an exponential decay function that mimics creep-induced stress redistribution; (iii) a selective power-law creep model is employed, in which different parameters are used depending on the level of deviatoric stress; and (iv) shale-specific empirical creep parameters are introduced. This enhanced model aims to bridge the gap between overly simplified analytical approaches and computationally intensive numerical simulations, offering a practical and insightful tool for evaluating long-term well integrity in P&A and CCS/CCUS) scenarios.

2 Methodology

This section presents the mathematical formulation of the analytical model and the numerical validation strategy used to benchmark its predictions. It also introduces the reference model that serves as the basis for both analytical and numerical analyses.

2.1 Reference model

The reference model adopted in all simulations presented in this work, both analytical and numerical, is a simplified version of the conceptual yet realistic vertical well models previously introduced by Morales-Monsalve and Fontoura [4], and Enayatpour et al. [5], as illustrated in Fig. 1. The well consists of a 12 1/4 inch borehole (diameter d_b= 31.115 cm), drilled with a mud weight of 10.1 ppg (equivalent to 11.9 kN/m³). The model represents a reservoir depth of 3820 m [4]. Two hypothetical casing sizes are considered: 9 5/8 inches (d_c = 24.4475 cm) and 10 3/4 inches (d_c = 27.305 cm) in diameter. Initial and boundary conditions applied in the model are presented in Fig. 1.

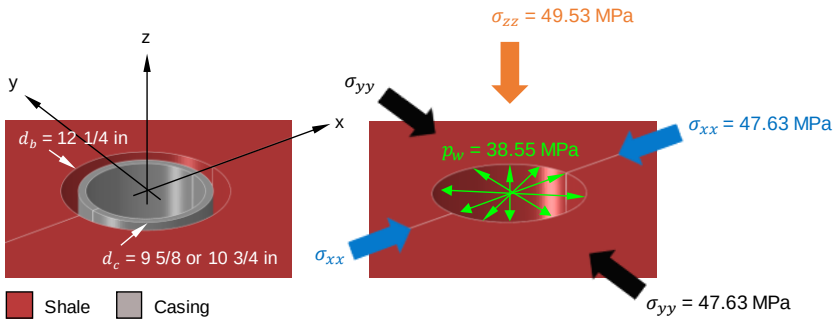


Figure 1. Conceptual well model. Geometry, and initial and boundary conditions based on refs. [4], [5].

2.2 Analytical solution

The analytical solution used to estimate time-dependent well closure in shale formations is an adapted version of Barker's original formulation proposed for salt steady-state creep [1]. Although developed for salt, the approach can be extended to clay-rich rocks through the appropriate calibration of creep parameters. In Barker's

original solution, creep deformation is driven by the difference between the far-field confining stress and the internal well pressure, referred to as the differential stress. In contrast, this study replaces that quantity with the Mises-type deviatoric stress q, which is more consistent with creep formulations commonly employed in numerical simulations. The deviatoric stress is computed using Eq. (1)**Error! Reference source not found.**, where σ_{ii} and σ_{ij} are the normal and shear stress components, respectively.

$$q = \sqrt{\frac{1}{2}\left(\left(\sigma_{xx} - \sigma_{yy}\right)^2 + \left(\sigma_{yy} - \sigma_{zz}\right)^2 + \left(\sigma_{zz} - \sigma_{xx}\right)^2\right) + 3\left(\sigma_{xy}{}^2 + \sigma_{yz}{}^2 + \sigma_{zx}{}^2\right)} \tag{1}$$

Furthermore, while salt formations often exhibit an isotropic geostatic stress state, which implies a null initial deviatoric stress, shale formations are generally transversely isotropic [6] and typically present an anisotropic in-situ stress condition. As a result, an initial deviatoric stress q_{geo} exists and may be considered as a threshold for the onset of creep, as supported by Souley et al. [7]. Although the replacement of the differential stress with the deviatoric stress has been previously implemented in the Elfen Well software (Rockfield) [8], the present work goes further by subtracting the initial deviatoric stress q_{geo}, calculated using Eq. (1), from the current deviatoric stress when calculating creep-induced displacements.

The post-drilling stress state is obtained from Kirsch's elastic solution for a plate with a circular hole subjected to internal and far-field pressures. This formulation is derived from the equilibrium equations in cylindrical coordinates under plane strain conditions. The well is assumed to be vertical, with vertical stress represented by σ_{zz}. The surrounding medium is considered elastic, linear and isotropic, allowing a closed-form solution. For a point located at a radial distance x and angular position β (in radians), the stresses are described according to Eq. (2). In this expression, σ_{ij} are the total far-field initial stresses (geostatic), R is the well radius and p_w is the internal well pressure. The deviatoric stress induced by drilling (q_{drill}), which shall trigger creep behavior, is then computed using Eq. (1) to the stress field derived from Eq. (2), subtracting the initial deviatoric stress q_{geo} to isolate the component responsible for creep activation.

$$\begin{Bmatrix}\sigma_{xx}\\ \sigma_{yy}\\ \sigma_{zz}\\ \sigma_{xy}\end{Bmatrix}_{drill} = \begin{Bmatrix}\left(\frac{\sigma_{xx}+\sigma_{yy}}{2}\right)\left(1-\left(\frac{R}{x}\right)^2\right)+\left(\frac{\sigma_{xx}-\sigma_{yy}}{2}\right)\left(1+3\left(\frac{R}{x}\right)^4-4\left(\frac{R}{x}\right)^2\right)\cos(2\beta)-p_w\left(\frac{R}{x}\right)^2\\ \left(\frac{\sigma_{xx}+\sigma_{yy}}{2}\right)\left(1-\left(\frac{R}{x}\right)^2\right)-\left(\frac{\sigma_{xx}-\sigma_{yy}}{2}\right)\left(1+3\left(\frac{R}{x}\right)^4\right)\cos(2\beta)+p_w\left(\frac{R}{x}\right)^2\\ 2v\left(\sigma_{xx}-\sigma_{yy}\right)\left(\frac{R}{x}\right)^2\cos(2\beta)\\ \left(\frac{\sigma_{yy}-\sigma_{xx}}{2}\right)\left(1-3\left(\frac{R}{x}\right)^4+2\left(\frac{R}{x}\right)^2\right)\text{sen}(2\beta)\end{Bmatrix} \tag{2}$$

After drilling, the creep behavior becomes active and initiates the gradual closure of the well. The time evolution of the well radius ($R(t)$) is governed by Eqs. (3) and (4), where R_0 is the initial well radius, and M is a steady-state creep coefficient that depends on the deviatoric stress, temperature (T) and empirical material parameters. The creep parameters A_i and n_i were calibrated based on experimental data from a reference clayey rock, the Callovo-Oxfordian (COx) claystone. The subscript i refers to the specific creep mechanism in action, which depends on the deviatoric stress level. A dedicated paper is under development by the authors documenting the creep constitutive model and parameter calibration. Furthermore, Q represents the activation energy for creep and R^* is the universal gas constant.

$$R(t) = R_0 \exp(-Mt) \tag{3}$$

$$M = \left(\frac{\sqrt{3}^{n_i+1}}{4n_i - 2}\right) A_i \exp\left(-\frac{Q}{R^* T}\right)\left(q^{n_i}\right) \tag{4}$$

In the original Barker solution, the differential stress is assumed to remain constant over time. However, it

is well established that creeping rocks such as salt and shale experience stress relaxation as a result of ongoing deformation. Consequently, the deviatoric stress gradually decreases with time. To account for this behavior in the analytical formulation, the temporal evolution of the deviatoric stress ($q(t)$) was approximated by an exponential decay function, as expressed in Eq. (5). In this expression, the coefficient 9757.4 represents the amplitude of the transient deviatoric component, $4.2452 * 10^{-5}$ is the exponential decay rate, and 6050 corresponds to the long-term asymptotic value of the stress. These parameters were calibrated based on the results of benchmark finite element simulations conducted at different temperatures. Accordingly, the deviatoric stress in Eq. (4) is updated at each time increment and adjusted by subtracting q_{geo}, thereby incorporating the effect of stress relaxation into the model.

$$q(t) = 9757.4 \exp(-4.2452 * 10^{-5}\, t) + 6050 \tag{5}$$

This modified analytical solution was implemented in Python using an explicit time-stepping scheme. The algorithm follows the sequence of steps previously described, and a summary of its structure is provided in the pseudocode presented in the analytical solution workflow shown in Fig. 2 (a).

3 Results

To evaluate the performance of the proposed modified analytical solution, comparative simulations were carried out. The simulations were organized into three scenarios, each differing in how the deviatoric stress evolves over time (Fig. 2 (b)). In scenario 1, the analytical solution considers the same deviatoric stress evolution obtained from the numerical simulator. Scenario 2 assumes that the initial deviatoric stress (immediately after excavation) remains constant throughout the entire simulation period, disregarding any stress relaxation caused by creep. Scenario 3 incorporates the exponential decay function defined in Eq. (5) to represent stress relaxation over time.

Each scenario was evaluated at five distinct temperatures: 20°C (low value assumption), 30.6°C [4], 40°C (intermediate value assumption), 54°C [5] and 76°C [9]. It is important to note that temperature directly influences creep rates (as seen in Eqs. (3) and (4)), which in turn affect deviatoric stresses magnitudes, since these are computed as a by-product of stress integration based on strain increments and the elastic constitutive matrix.

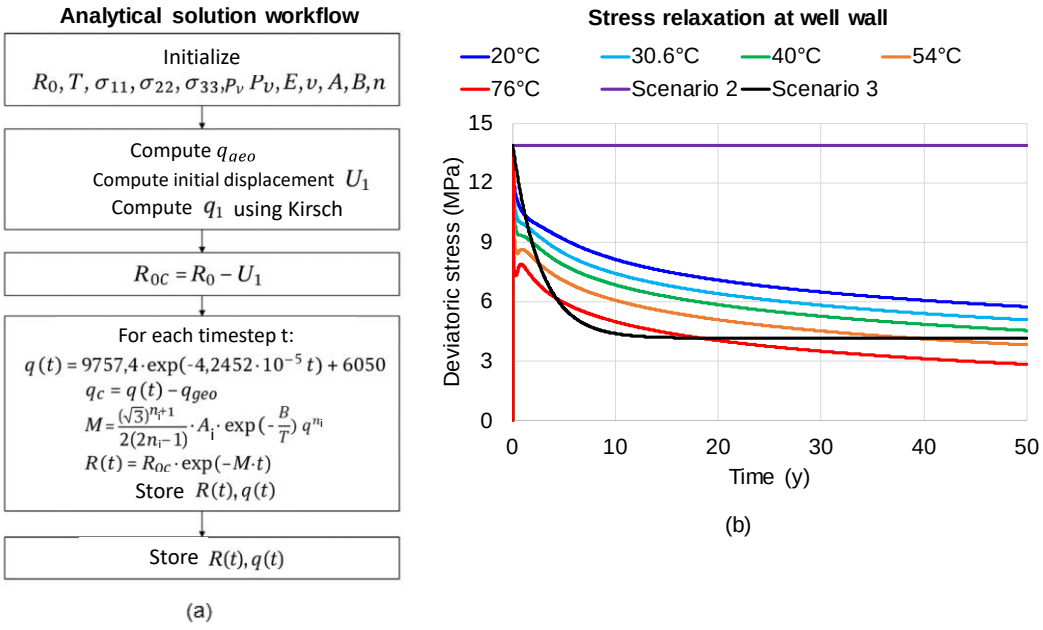


Figure 2. (a) Analytical solution workflow and (b) different approaches for the deviatoric stresses over time.

All simulations assume the same geometric configuration, material parameters, and a constant well pressure. The evolution of the well radius and over a 50-year period was calculated and compared against finite element simulations carried out in ABAQUS®. This benchmarking effort serves both to validate the analytical model and to assess its predictive capability across a temperature range representative of conditions from near-surface to Pre-salt depths. Notably, shales with potential for forming geological barriers in the P&A of Brazilian wells are expected to operate within this temperature interval, highlighting the importance of evaluating thermal sensitivity in long-term well integrity predictions.

Figure 3 presents the evolution of the well diameter over time for the five temperature levels and the three previously described scenarios. Results from the modified analytical model are represented by solid curves, while the corresponding finite element simulation results are shown as dashed curves, allowing for direct comparison across all cases.

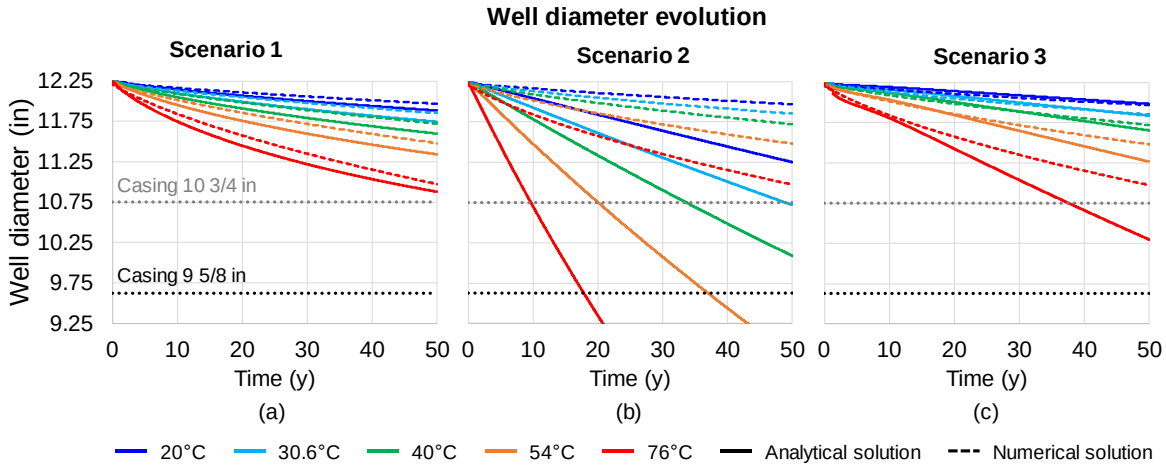


Figure 3. Well diameter over time of scenarios 1 (a), 2 (b) and 3 (c). Solid, dashed and dotted curves represent respectively analytical and numerical solutions, and casing diameters.

Figure 3 (a) shows the results of Scenario 1, in which the analytical model uses the same time-dependent deviatoric stress evolution as obtained from the numerical simulation (Fig. 2 (b)). At 20 °C, the formation undergoes minimal creep, and the analytical prediction closely follows the finite element results, indicating a very gradual reduction in well diameter. As the temperature increases to 30.6 °C, the rate of deformation slightly increases, but both approaches still show excellent agreement over the 50-year period. At 40 °C, the well experiences more pronounced closure, with the analytical model continuing to replicate the trend observed in the numerical results. At 54 °C, the deformation accelerates significantly, yet the solid and dashed curves remain very close. At 76 °C (red curves), the analytical and numerical predictions still align well, even as the well diameter approaches critical casing thresholds. Overall, Scenario 1 highlights the strong accuracy of the analytical model when the deviatoric stress evolution is prescribed from finite element results. If a casing of 10 3/4 inches (in nominal diameter) were considered, the barrier would not form in either model i.e. the curves do not reach the horizontal line that represents the casing.

Figure 3 (b) presents the results of Scenario 2, where the initial deviatoric stress is assumed constant over time, with no stress relaxation considered. At 20 °C, the predictions already overestimate the numerical simulation by about 3/4 inch, as time-dependent deformation is limited. At 30.6 °C, the analytical model overestimates the well closure by more than one inch compared to the finite element approach. At 40 °C, the gap between the two solutions becomes more evident, with the analytical model predicting faster closure. With the temperature raised to 54 °C, the analytical curves diverge significantly, anticipating a much faster reduction in diameter than observed numerically. At 76 °C (red curves), the analytical model shows rapid and severe closure, with the diameter falling below the casing threshold well before 20 years, while the numerical simulation indicates a more gradual response. These results confirm that neglecting stress relaxation can lead to unrealistic and overly conservative predictions of long-term deformation, predicting barrier formations (from T = 30.6°C on) around the casings of 10 3/4 and 9 5/8 inches not corroborated by the numerical simulations.

Figure 3 (c) shows the results of Scenario 3, in which stress relaxation is incorporated through the

exponential decay function. At 20 °C, the formation exhibits limited time-dependent deformation. The analytical model predicts a slow reduction in the well diameter over the 50-year simulation period, with minimal deviation from the numerical results. As temperature increases to 30.6 °C, the creep rate becomes slightly more pronounced, and well closure accelerates moderately, though the analytical and numerical predictions remain closely aligned. At 40 °C, the deformation becomes more significant, with both approaches indicating a steady decline in diameter over time. At 54 °C, the impact of temperature is clearly amplified, leading to a more rapid closure trend, while the analytical model continues to capture the response with good accuracy. At 76 °C (red curves), the results confirm the strong influence of temperature on accelerating time-dependent deformation, with the well diameter approaching the threshold of the casing of 10 3/4 inches more quickly, indicating the barrier formation. The corresponding numerical simulation provides smaller displacements than the analytical solution, and the well diameter numerical curve did not reach the line of the casing of 10 3/4 inches. However, the overall behavior was more compatible with the numerical simulations. In general, Scenario 3 demonstrates that incorporating stress relaxation through a calibrated decay function enhances the analytical model's ability to predict long-term well behavior under thermally activated creep conditions.

4 Discussion

The proposed methodology bridges the gap between fully empirical formulations and computationally demanding numerical models. Overall, the analytical model demonstrates strong performance effectively capturing the interplay between stress redistribution and well closure over time also considering the temperature contribution. In addition to its accuracy, the approach offers a clear advantage in terms of computational efficiency. While finite element models deliver detailed spatial resolution and can incorporate complex material behavior, they require significant computational resources and specialized expertise. In contrast, the analytical solution developed in this study achieves comparable predictive capability with drastically reduced simulation time, making it a practical and efficient tool for preliminary evaluations, parametric studies, and large-scale field applications related to well integrity and P&A.

Nevertheless, certain assumptions and inherent limitations must be acknowledged. The analytical formulation is based on radial symmetry and linear elasticity for the initial stress state. It adopts a simplified representation of the steady-state creep that does not account for local heterogeneities, anisotropy, or coupled thermo-hydro-mechanical interactions typically present in real geologic formations. Still, temperature is explicitly treated as a state variable within the creep constitutive model, allowing thermal effects to influence time-dependent deformation behavior.

Despite these simplifications, the model's ability to reproduce nonlinear, time-dependent trends with high fidelity supports its potential integration into broader well integrity and P&A workflows. In particular, its simplicity, flexibility, and speed make it well suited for risk assessment frameworks and for supporting the design of long-term shale barriers in wells.

5 Conclusions

This study introduced a modified and enhanced analytical solution for predicting well closure driven by creep deformation in shale formations in the context of plug and abandonment (P&A). Departing from classical formulations that assume constant differential stress and are tailored to salt formations, the proposed model reformulates Barker's solution by incorporating a deviatoric stress relaxation function calibrated from finite element simulations. This enhancement allows for a more accurate representation of the creep behavior of shale while preserving the efficiency and tractability of a closed-form analytical approach.

The main contributions of this work include: (i) the integration of an exponentially decaying deviatoric stress profile into an analytical creep framework, (ii) validation of the methodology through direct comparison with numerical simulations, and (iii) systematic assessment of temperature effects on long-term well integrity. The model consistently reproduced the numerical results across a wide range of temperatures, capturing the transition from minimal deformation at 20 °C to rapid closure at 76 °C.

This analytical methodology offers a robust and computationally efficient tool for the early-stage design and screening of P&A strategies, particularly when time or computational resources are limited. It also provides

a foundation for integration into broader workflows for risk evaluation, sensitivity studies, and regulatory compliance.

Future developments should focus on extending the formulation to account for anisotropic mechanical behavior, pressure transients, and three-dimensional features such as bedding planes. Additionally, coupling this model with in-situ monitoring data and machine learning techniques could expand its use toward real-time field diagnostics and adaptive abandonment planning.

Acknowledgements. This research was carried out in association with the ongoing R&D project registered as ANP no. 23659-6, "SABAR" (PUC-Rio/Petrobras/ANP) sponsored by Petrobras under the ANP R&D levy, Brazil as "Compromisso de Investimentos com Pesquisa e Desenvolvimento".

Authorship statement. The authors hereby confirm that they are the sole liable persons responsible for the authorship of this work, and that all material that has been herein included as part of the present paper is either the property (and authorship) of the authors, or has the permission of the owners to be included here.

References

[1] J. W. Barker, K. W. Feland, and Y. H. Tsao, "Drilling long salt sections along the U.S. Gulf Coast," *SPE Drill. Complet.*, vol. 9, no. 3, pp. 185–188, 1994, doi: 10.2118/24605-pa.

[2] R. E. Goodman, *Introduction to Rock Mechanics*, 2nd ed. John Wiley & Sons, 1989.

[3] E. Fjær, R. M. Holt, P. Horsrud, A. M. Raaen, and R. Risnes, *Petroleum Related Rock Mechanics*. Elsevier B.V., 2021. doi: 10.1016/B978-0-12-822195-2.00002-4.

[4] C. B. Morales-Monsalve and S. A. B. Fontoura, "Numerical solution of wellbore closure due to shale creep: a poro-visco-elastoplastic approach," *SSRN*, 2023, doi: http://dx.doi.org/10.2139/ssrn.4538137.

[5] S. Enayatpour, A. Thombare, M. Aldin, and E. van Oort, "Exploiting shale creep deformation to create annular barriers for well plugging and abandonment: Experimental investigation and numerical simulation," in *SPE Annual Technical Conference and Exhibition*, Calgary: Society of Petroleum Engineers (SPE), 2019. doi: 10.2118/195966-ms.

[6] C. L. Zhang, G. Armand, N. Conil, and B. Laurich, "Investigation on anisotropy of mechanical properties of Callovo-Oxfordian claystone," *Eng. Geol.*, vol. 251, pp. 128–145, 2019, doi: 10.1016/j.enggeo.2019.02.008.

[7] M. Souley *et al.*, "A Regularised Anisotropic Elastoplastic Damage and Viscoplastic Model and Its Hydromechanical Application to a Meuse/Haute-Marne URL Drift," *Rock Mech. Rock Eng.*, vol. 57, pp. 4389–4419, 2024, doi: 10.1007/s00603-023-03563-1.

[8] Rockfield, "Comparison of a Creep-Only Wellbore Model with an Analytical Creep Solution," *Elfen wellbore*, 2023. https://www.rockfieldglobal.com/blog/comparison-creep-only-wellbore-model-analytical-creep-solution/

[9] P. A. L. P. Firme, D. Roehl, C. Mejia, and C. Romanel, "Geomechanics of salt towards natural barriers for the abandonment of pre-salt wells in Brazil," *Geoenergy Sci. Eng.*, vol. 228, p. 211849, 2023, doi: 10.1016/j.geoen.2023.211849.